



## Geochemical Analysis of Groundwater in Central Cross River State: Implications for Water Quality and Public Health

<sup>1</sup>Eteng Ebri, <sup>1</sup>Nsikak Bassey, <sup>2</sup>Nyakno Jimmy George, <sup>2</sup>Thomas Harry

Received: January 21, 2025 / Accepted: March 22, 2025

© REJOST 2025

### Abstract

Groundwater quality in Central Cross River State, Nigeria, is vital for public health and sustainability. This study evaluates the geochemical characteristics of groundwater in parts of the central Cross River State within the Ikom-Mamfe Embayment, analyzing physicochemical parameters, major ions, trace metals, and correlation matrix analysis. A total of 23 boreholes were sampled, revealing pH values between 6.17 and 8.50 (mean: 6.87) and electrical conductivity (EC) ranging from 28.67 to 198.50  $\mu\text{S}/\text{cm}$  (mean: 133.43  $\mu\text{S}/\text{cm}$ ). Major anions include chloride ( $\text{Cl}^-$ ) at 0.25–5.10 mg/L (mean: 1.74 mg/L), fluoride ( $\text{F}^-$ ) at 0.03–0.21 mg/L (mean: 0.13 mg/L), nitrate ( $\text{NO}_3^-$ ) at 0.10–2.00 mg/L (mean: 0.91 mg/L), nitrite ( $\text{NO}_2^-$ ) at 0.01–1.10 mg/L (mean: 0.16 mg/L), and sulfate ( $\text{SO}_4^{2-}$ ) at 4.50–7.20 mg/L (mean: 5.85 mg/L), all within WHO limits. Major cations include calcium carbonate ( $\text{CaCO}_3$ ) at 11.00–376.00 mg/L (mean: 134.71 mg/L), iron ( $\text{Fe}^{2+}$ ) at 3.05–6.23 mg/L (mean: 4.44 mg/L), magnesium ( $\text{Mg}^{2+}$ ) at 0.10–0.49 mg/L (mean: 0.16 mg/L), manganese ( $\text{Mn}^{2+}$ ) at 0.10–0.32 mg/L (mean: 0.16 mg/L), and sodium ( $\text{Na}^+$ ) at 1.10–1.41 mg/L (mean: 1.14 mg/L). Hydrogeochemical facies analysis (Piper and Durov diagrams) classifies groundwater as predominantly Ca- $\text{HCO}_3$  type, indicating carbonate dissolution as a key influence. Correlation matrix analysis revealed strong associations between EC and major cations/anions, highlighting mineral dissolution as a primary control on groundwater chemistry. Negative correlations between pH and  $\text{Fe}^{2+}$  (-0.453) and  $\text{Mn}^{2+}$  (-0.045) suggest that lower pH levels increase metal solubility, while positive correlations between turbidity and  $\text{Fe}^{2+}$  (0.354) indicate potential contamination sources. Elevated  $\text{Fe}^{2+}$  and  $\text{Mn}^{2+}$  concentrations exceed WHO drinking water guidelines, posing health risks. While groundwater remains largely suitable for irrigation, localized anthropogenic contamination

from agriculture and waste disposal necessitates improved monitoring, pollution control, and targeted water treatment strategies. Sustainable groundwater management policies are essential to ensure long-term water safety in the region.

✉ Thomas A. Harry: [tharry.tom@gmail.com](mailto:tharry.tom@gmail.com)

<sup>1</sup>Department of Geology, Akwa Ibom State University

<sup>2</sup>Department of Physics, Geophysics Research Group, Akwa Ibom State University

**Keywords:** Groundwater quality, Hydrogeochemistry, Water contamination, Correlation matrix, Central Cross River State, Public health, Piper diagram, Water management.

## 1.0 Introduction

Ensuring access to safe drinking water is a critical component of public health and sustainable resource management (Gandla *et al.*, 2024; Ibanga & George, 2016; Umoh *et al.*, 202a, 2022b). Groundwater is the primary drinking water source for communities in Central Cross River State, Nigeria, making its quality a major public health concern. However, groundwater is susceptible to contamination from both natural and anthropogenic sources (Thomas *et al.*, 2020; Udosen *et al.*, 2024). The region's geology, characterized by sedimentary formations, plays a significant role in shaping the hydrogeochemical composition of groundwater, while human activities such as agriculture, waste disposal, and industrialization further contribute to contamination (George & Thomas, 2023).

The study area falls within the Ikom-Mamfe Embayment, which is part of the larger sedimentary basins of southeastern Nigeria. The embayment is composed of Cretaceous and Tertiary sedimentary sequences dominated by sandstone, shale, and limestone lithologies. The Mamfe Formation, which is a major lithostratigraphic unit in this area, consists predominantly of ferruginous sandstones and shales, interbedded with limestone lenses (Akpan *et al.*, 2013). These lithological units influence groundwater chemistry through natural weathering and dissolution processes (Obiora *et al.*, 2016; Inyang *et al.*, 2023). The presence of ferruginous formations is a key contributor to elevated iron (Fe) and manganese

(Mn) levels in some groundwater sources (Akpan *et al.*, 2018).

In addition to geological influences, human activities such as extensive farming, urbanization, and improper waste disposal exacerbate groundwater contamination risks (Bassey *et al.*, 2013). Agricultural practices involving excessive fertilizer application introduce high nitrate ( $\text{NO}_3^-$ ) concentrations into groundwater, while waste leachates and septic systems contribute to bacterial and chemical contamination (Inim *et al.*, 2020).

Having the mechanistic understanding of the geochemical characteristics of groundwater is essential for assessing its suitability for consumption and developing strategies to mitigate contamination risks (Ekanem *et al.*, 2021). This study seeks to analyze the physicochemical properties of groundwater in the region, evaluate contamination risks, and propose measures to enhance water safety.

## 1.1 Study Location, geology and hydrogeology

The region in Figure 1 shows the map of the study area lying between latitudes  $5^{\circ}30'N$  and  $6^{\circ}15'N$  and longitudes  $7^{\circ}45'E$  and  $9^{\circ}00'E$  and is part of the Central Cross River State, South-South Nigeria. It experiences a sub-equatorial climate, with annual rainfall exceeding 300 cm and temperatures ranging from  $21.9^{\circ}C$  to  $31.7^{\circ}C$  (Akpan *et al.*, 2013). The study area is situated within the Ikom-Mamfe Embayment, a geological setting that significantly influences groundwater occurrence and quality. The

geology comprises formations of the Eze-Aku Group, Nkporo Shales, and basaltic intrusions, which significantly influence groundwater occurrence and quality. While these formations

host aquifers with substantial water potential, their hydrogeochemical interactions often affect water quality, making it unsuitable for human consumption.

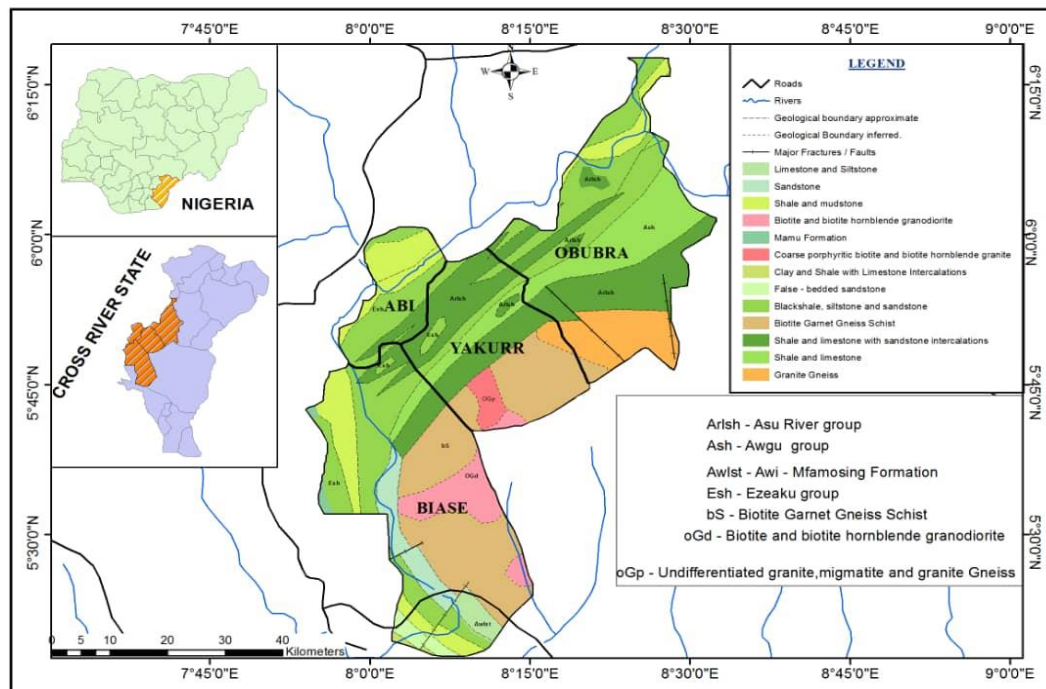


Figure 1: Geology Map of the Study Area

## 2.0 Quality of groundwater in the area

Groundwater quality is influenced by both geogenic and anthropogenic factors (Gandla *et al.*, 2024). Lithological characteristics significantly affect groundwater chemistry, as the presence of minerals such as feldspars, carbonates, and sulfates determine the ion concentrations in groundwater (Hem, 1985). Additionally, human activities, including agricultural practices and industrial discharges, have been linked to increased contamination levels (George *et al.*, 2021; WHO, 2022).

Several studies have been conducted within the Ikom-Mamfe Embayment, focusing on hydrogeochemistry, water resource management, and contamination pathways. Previous research by Okon *et al.* (2018) indicated that groundwater in the region exhibits high variability in electrical conductivity and total dissolved solids, largely attributed to geological heterogeneity. Similarly, Ekwere and

Ekwueme (2016) identified significant contributions of anthropogenic contaminants, particularly from agricultural runoff and domestic sewage, to groundwater quality deterioration in parts of Central Cross River State.

Hydrogeochemical facies classification has proven effective in evaluating water quality in similar geological settings (Piper, 1944; Durov, 1948). Furthermore, groundwater vulnerability assessments have highlighted the significance of pollution index models in determining contamination levels (APHA, 2017). This study builds on these previous findings by applying hydrogeochemical techniques to analyze groundwater quality in Central Cross River State.

## 3. Methodology

### 3.1 Sample Collection

Groundwater samples were collected from systematically selected boreholes (23) to ensure

representative spatial distribution and geological variations (Figure 2). Standardized sampling techniques were employed to maintain data reliability and accuracy. Boreholes were chosen based on proximity to potential contamination sources, including agricultural farmlands, residential settlements, and industrial zones.

### 3.2 Laboratory Analysis

Using standard laboratory and field equipment, along with well-documented methodologies from the literature, the physicochemical parameters listed in Table 3.1 were measured and analyzed either in the field or in the laboratory, as appropriate.

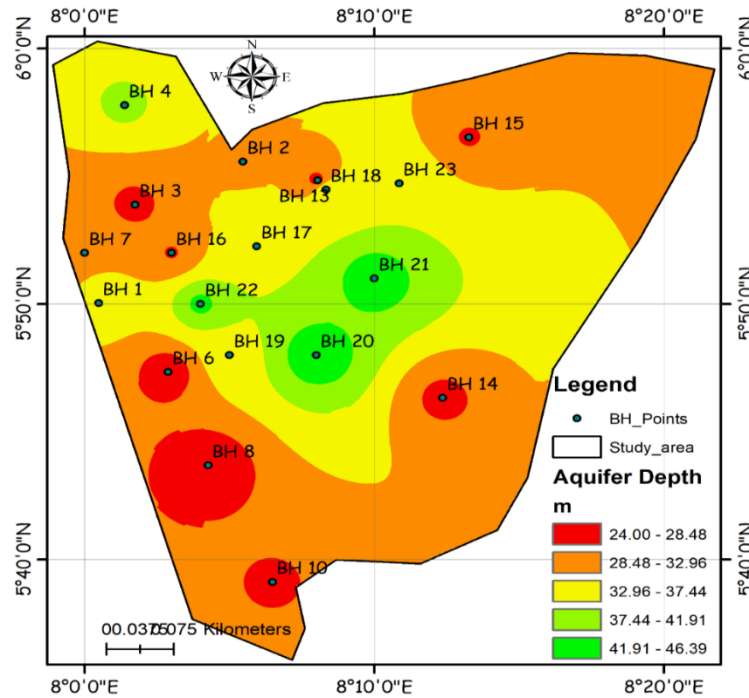


Figure 2: Spatial map of aquifer depth showing Borehole locations within the study area

Table 1: Physicochemical parameters and method of analysis

Parameter	Method of Analysis
pH	pH meter
Electrical Conductivity	Conductivity meter
Total Dissolved Solids (TDS)	Gravimeter Analysis
Major Cations (Ca <sup>2+</sup> , Mg <sup>2+</sup> , Na <sup>+</sup> , K <sup>+</sup> )	Flame Photometry and Atomic Absorption Spectrophotometry (AAS)
Major Anions (Cl <sup>-</sup> , SO <sub>4</sub> <sup>2-</sup> , NO <sub>3</sub> <sup>-</sup> , HCO <sup>-</sup> )	Chromatography
Ion	
Heavy Metals (Fe, Mn, Pb, Zn)	Atomic Absorption Spectrophotometry (AAS)
Salinity and Specific Gravity	Hydrometer

Additional work conducted includes hydrogeochemical analysis to evaluate groundwater recharge sources and contaminant transport mechanisms. Previous studies in the region have employed Piper plots, correlation matrix analysis, and hydrochemical characterization to assess groundwater quality

and identify key geochemical processes influencing water composition. By integrating these analytical techniques, this study provides valuable insights into groundwater sustainability and public health protection in the region.

## 4.0 Results

### 4.1 Physical Parameters

This section examines the spatial variability and quality of borehole water across various locations, focusing on parameters such as temperature, turbidity, pH, and electrical conductivity (EC). The findings offer critical

insights into water suitability, emphasizing compliance with standard regulatory requirements (Uka et al., 2019). Table 4.1 presents a comprehensive summary of the data, while spatial maps (Figures 3 to 6) visually depict the trends and distribution patterns of these parameters.

**Table 2:** Borehole Water Quality Parameters

Code	Temperature (°C)	Turbidity (NTU)	pH	EC (µS/cm)	Remarks
BH 1	27.00	18.00	6.30	132.70	Low salinity (good for irrigation)
BH 2	27.30	17.00	6.50	118.80	Low salinity (good for irrigation)
BH 3	25.23	22.00	6.85	108.30	Low salinity (good for irrigation)
BH 4	25.00	18.80	6.90	184.00	Low salinity (good for irrigation)
BH 5	27.60	19.70	6.20	112.20	Low salinity (good for irrigation)
BH 6	27.00	17.30	7.10	115.40	Low salinity (good for irrigation)
BH 7	30.60	21.70	6.29	164.09	Low salinity (good for irrigation)
BH 8	30.51	19.60	6.17	115.40	Low salinity (good for irrigation)
BH 9	30.51	19.60	6.17	115.40	Low salinity (good for irrigation)
BH 10	30.51	19.60	6.17	115.40	Low salinity (good for irrigation)
BH 11	27.40	18.20	6.50	133.20	Low salinity (good for irrigation)
BH 12	26.70	18.30	6.30	112.20	Low salinity (good for irrigation)
BH 13	25.40	16.60	6.20	175.30	Low salinity (good for irrigation)
BH 14	26.20	17.30	6.50	170.50	Low salinity (good for irrigation)
BH 15	25.40	16.60	7.20	175.30	Low salinity (good for irrigation)
BH 16	26.90	14.20	6.90	198.50	Low salinity (good for irrigation)
BH 17	27.40	16.30	6.85	188.70	Low salinity (good for irrigation)
BH 18	27.40	18.70	6.50	188.67	Low salinity (good for irrigation)
BH 19	27.40	17.50	6.85	88.20	Low salinity (good for irrigation)
BH 20	26.20	15.00	8.50	62.80	Low salinity (good for irrigation)
BH 21	26.20	18.30	8.40	52.10	Low salinity (good for irrigation)
BH 22	28.20	17.00	8.20	112.20	Low salinity (good for irrigation)
BH 23	29.00	16.00	8.00	28.67	Low salinity (good for irrigation)

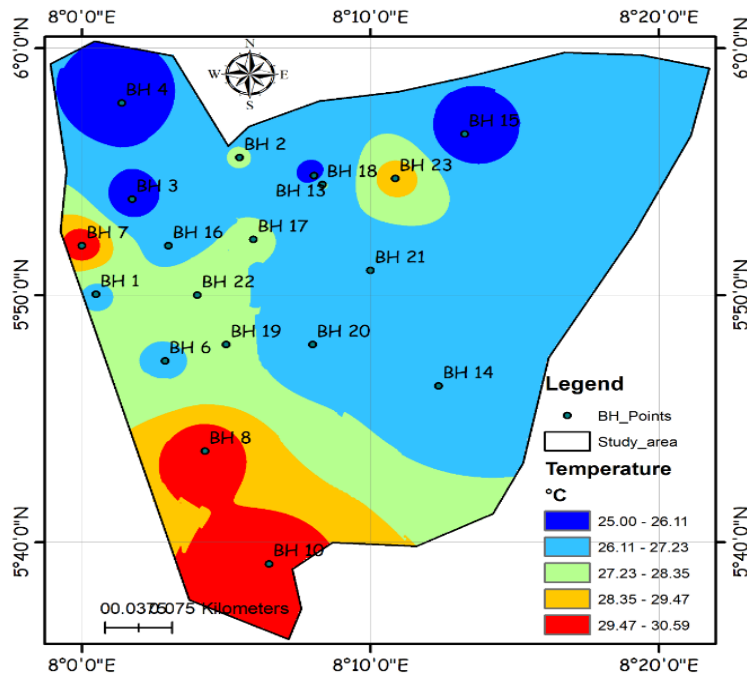


Figure 3: Spatial map of borehole water temperature in the Study Area

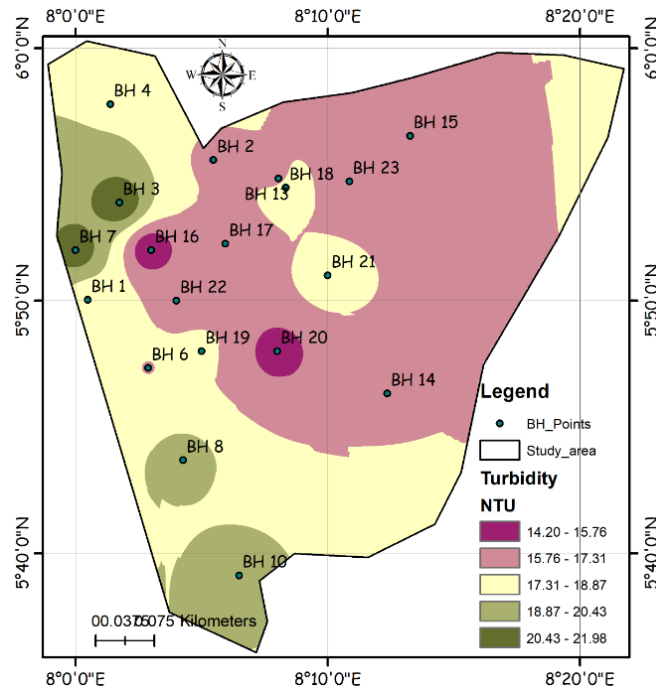


Figure 4: Spatial map of borehole water turbidity in the Study Area

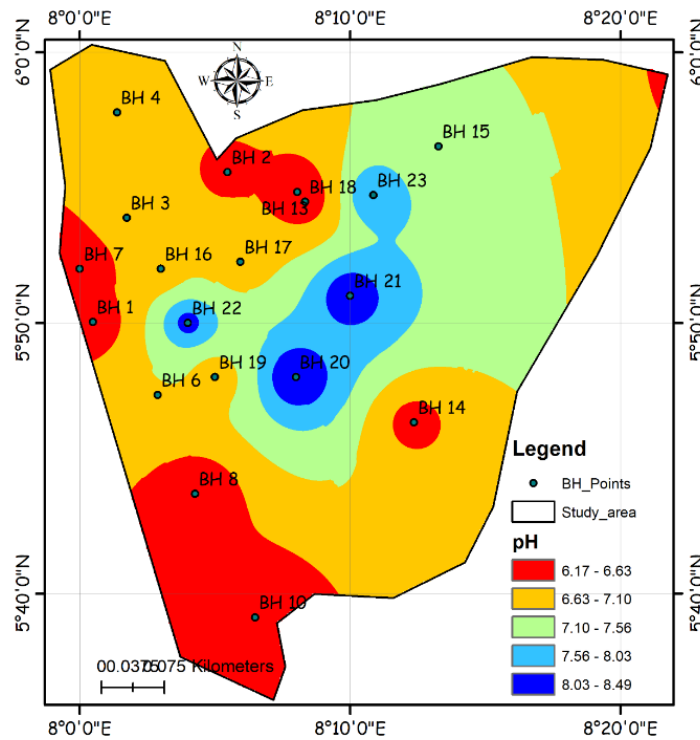


Figure 5: Spatial map of borehole water pH in the Study Area

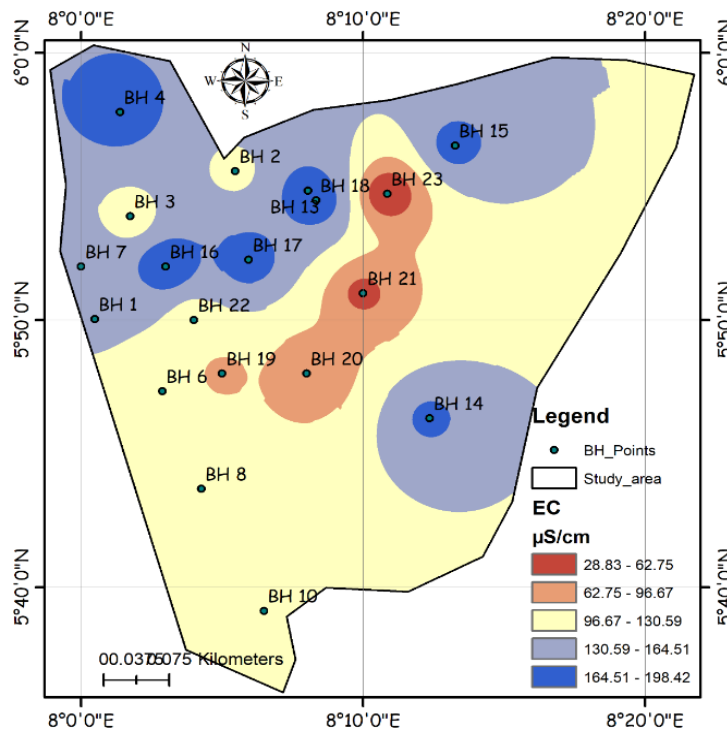


Figure 6: Spatial map of borehole water electrical conductivity in the Study Area

#### 4.2 Hydrochemical (major anions) Analysis of borehole water

The assessment focuses on chloride ( $\text{Cl}^-$ ), fluoride ( $\text{F}^-$ ), nitrate ( $\text{NO}_3^-$ ), and sulfate ( $\text{SO}_4^{2-}$ ). Table 3 summarizes the results, including the

standards recommended by the World Health Organization (WHO). Spatial maps (Figures 7 to 10) provide a visual interpretation of these parameters, aiding in understanding their distribution and potential environmental or anthropogenic influences.

**Table 3:** Hydrochemical (Major Anions) Composition of Borehole Water Compared to WHO Standards

Parameter	Range (mg/L)	Mean $\pm$ SD (mg/L)	WHO Standard (mg/L)	Remarks
Chloride (Cl <sup>-</sup> )	0.25–5.10	1.74 $\pm$ 1.08	250	Within acceptable range for irrigation
Fluoride (F <sup>-</sup> )	0.03–0.21	0.13 $\pm$ 0.05	1.5	Safe for irrigation and human health
Nitrate (NO <sub>3</sub> <sup>-</sup> )	0.10–2.00	0.91 $\pm$ 0.60	50	No risk to crops or groundwater
Nitrite (NO <sub>2</sub> <sup>-</sup> )	0.01–1.10	0.16 $\pm$ 0.22	3	Safe and unlikely to cause toxicity
Sulfate (SO <sub>4</sub> <sup>2-</sup> )	4.50–7.20	5.85 $\pm$ 0.88	500	Excellent for agricultural use

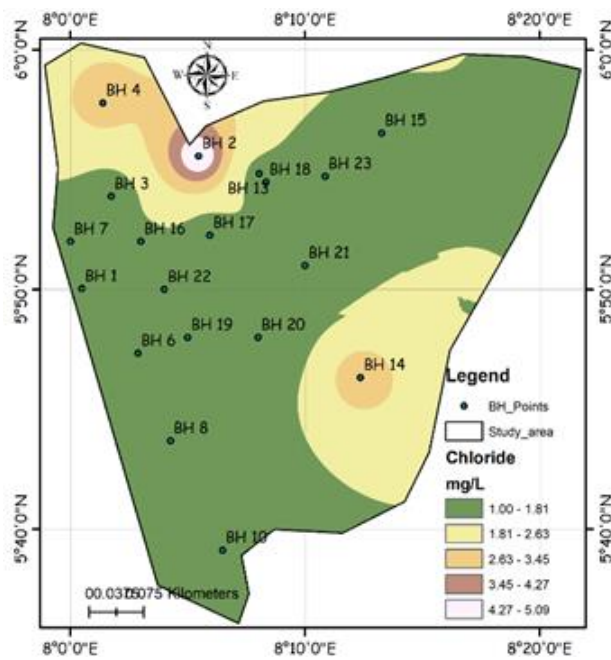


**Figure 7:** Spatial map of borehole water chloride concentration in the Study Area

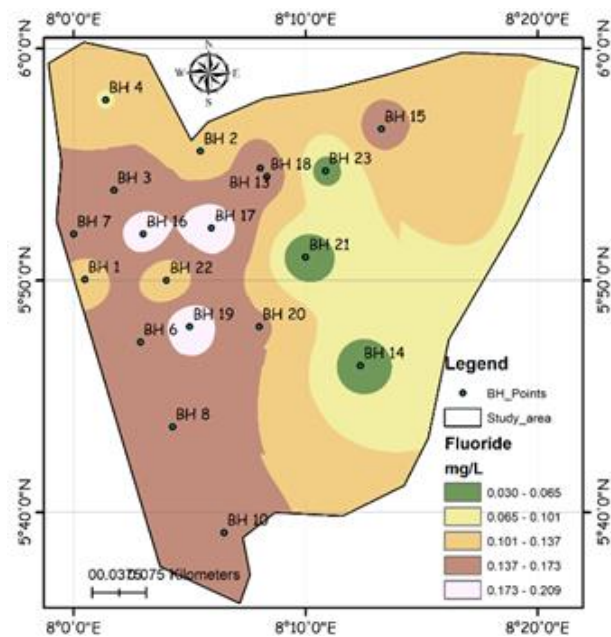


**Figure 8:** Spatial map of borehole water Fluoride concentration in the Study Area

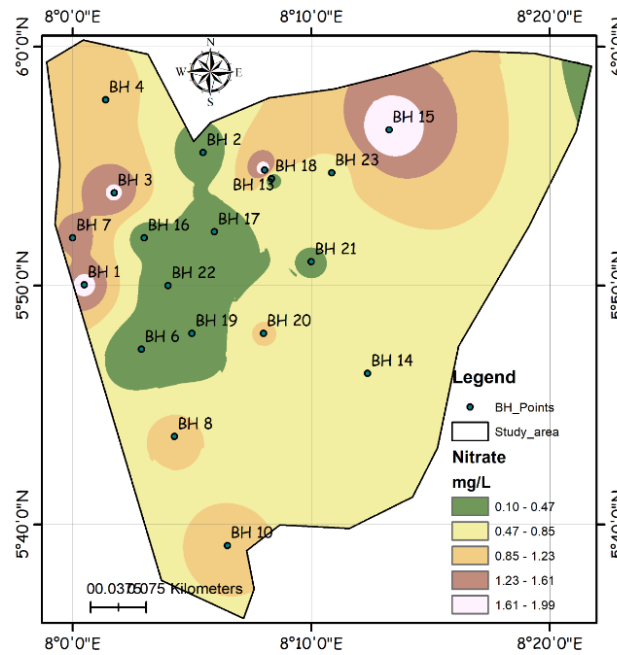


Figure 9: Spatial map of borehole water Nitrate concentration in the Study Area

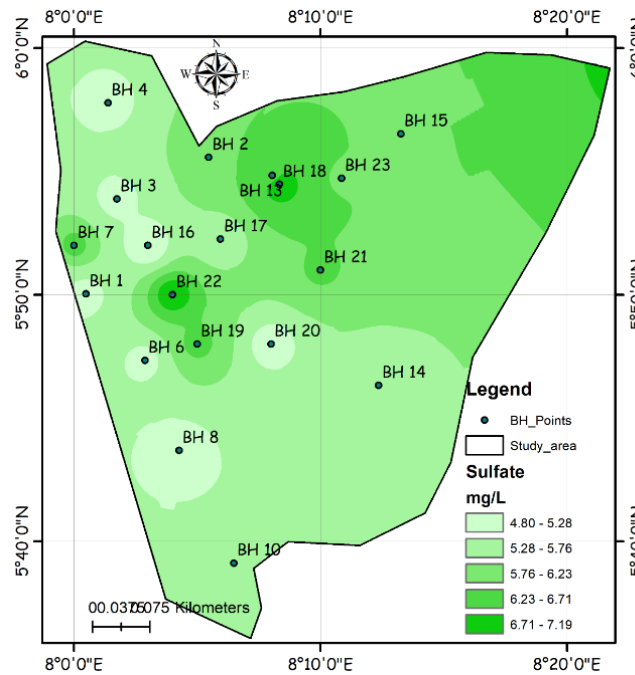


Figure 10: Spatial map of borehole water sulfate concentration in the Study Area

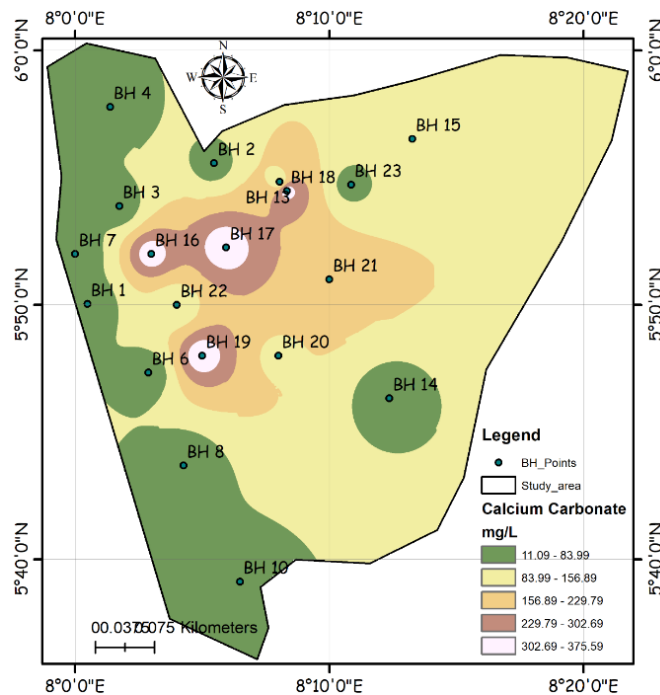
#### 4.3 Hydrochemical composition (major cations) and its implications for water quality

A comprehensive analysis of the hydrochemical composition (Major Cations) of borehole water from various locations within the study area. The parameters analyzed (Table 4) included Calcium Carbonate ( $\text{CaCO}_3$ ), Iron ( $\text{Fe}^{2+}$ ), Magnesium ( $\text{Mg}^{2+}$ ), Manganese ( $\text{Mn}^{2+}$ ), and Sodium ( $\text{Na}^+$ ), which are crucial in determining the suitability

of water for agricultural and other uses. These ions play significant roles in water chemistry, influencing both soil quality and the health of plants irrigated with this water (Duoxun *et al.*, 2023; Etesin *et al.*, 2023). By assessing the spatial distribution of these parameters (Figures 11 to 15), we can gauge their potential impact on irrigation practices, soil health, and crop productivity.

**Table 4:** Hydrochemical Composition (Major Cations) of Borehole Water

Borehole Location	Code	CaCO <sub>3</sub> (mg/L)	Fe <sup>2+</sup> (mg/L)	Mg <sup>2+</sup> (mg/L)	Mn <sup>2+</sup> (mg/L)	Na <sup>+</sup> (mg/L)
Usumutong	BH 1	11.00	3.27	0.70	0.93	1.21
Adadama	BH 2	40.38	5.05	0.10	0.27	1.10
Anong	BH 3	29.60	4.09	0.20	0.32	1.10
Ebom	BH 4	28.00	6.07	0.29	0.15	1.41
Ikpalegwa	BH 5	22.50	5.05	0.10	0.10	1.10
Imabana	BH 6	21.00	5.05	0.10	0.10	1.10
Itigidi	BH 7	18.00	4.50	0.15	0.10	1.10
Abini	BH 8	18.00	6.05	0.10	0.10	1.10
Agwuagune	BH 9	18.00	5.05	0.10	0.10	1.10
Etono	BH 10	41.07	4.05	0.10	0.10	1.10
Ababene	BH 11	26.00	6.23	0.49	0.20	1.13
Apiapum	BH 12	85.00	4.05	0.10	0.10	1.10
Isabang	BH 13	96.00	4.50	0.15	0.10	1.10
Ogada	BH 14	36.00	4.05	0.10	0.30	1.10
Ovukwa	BH 15	96.00	3.50	0.15	0.10	1.10
Akugom, Ugep	BH 16	356.00	4.05	0.10	0.10	1.10
Genong, Obioko-Ijiman	BH 17	376.00	3.05	0.10	0.30	1.10
Idomi	BH 18	350.38	5.01	0.15	0.10	1.10
Ijiman - Ugep	BH 19	367.00	4.05	0.10	0.30	1.10
Mkpani	BH 20	136.00	3.05	0.28	0.30	1.10
Nko	BH 21	216.00	3.16	0.15	0.20	1.10
NtankpoUgep	BH 22	85.00	4.05	0.10	0.10	1.10
Ugep	BH 23	52.00	4.26	0.10	0.10	1.10

**Figure 11:** Spatial map of borehole water Calcium carbonate concentration in the Study Area

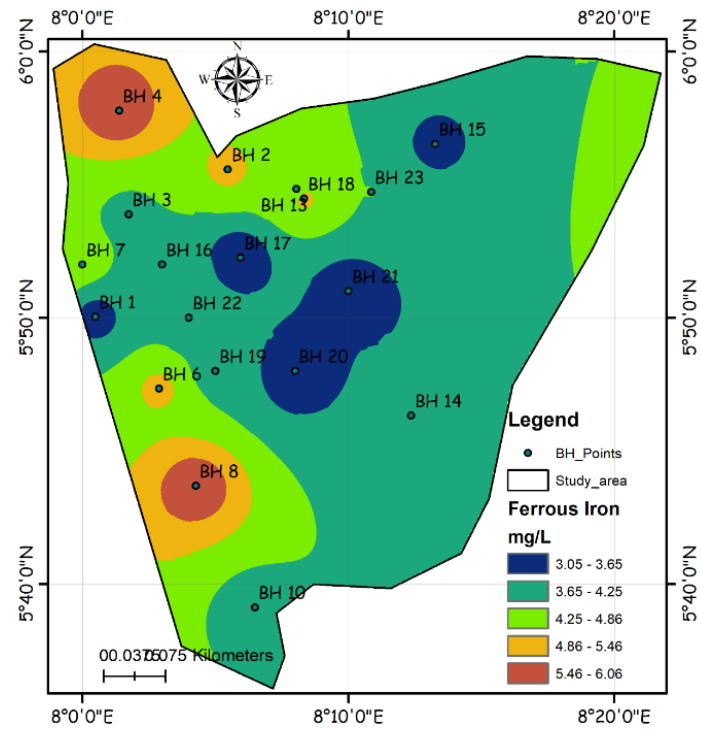


**Figure 12:** Spatial map of borehole water Iron concentration in the Study Area

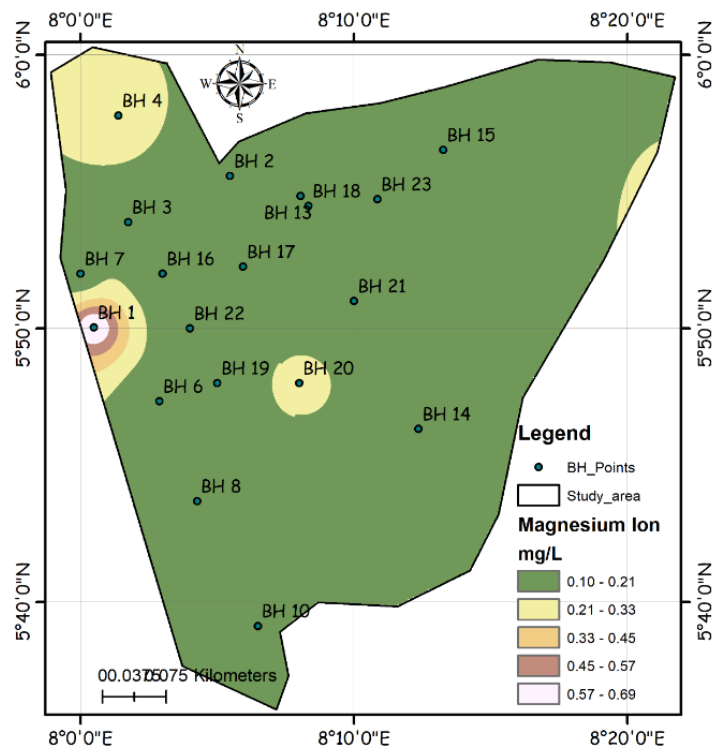


**Figure 13:** Spatial map of borehole water Magnesium concentration in the Study Area

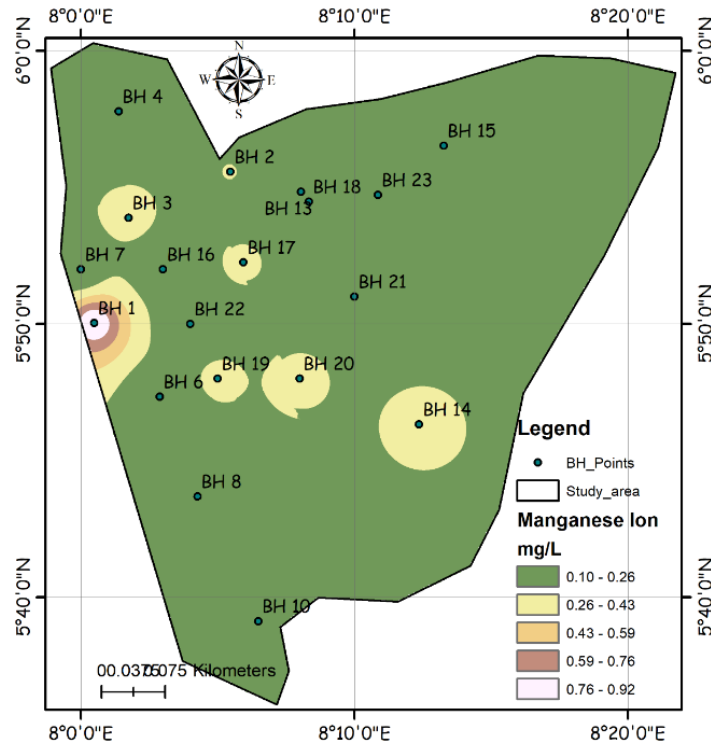


Figure 14: Spatial map of borehole water Manganese concentration in the Study Area

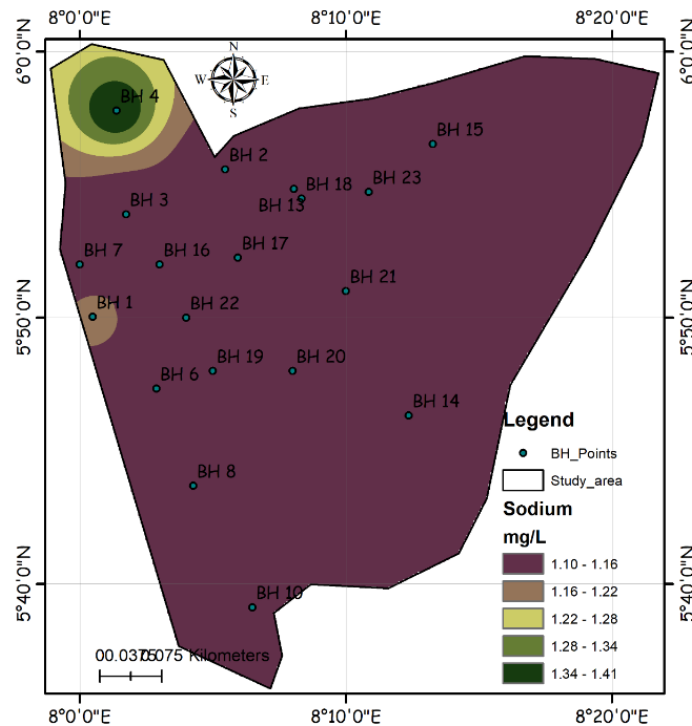


Figure 15: Spatial map of borehole water Sodium concentration in the Study Area

**4.4 Correlation Matrix Analysis**

Figure 16 presents the Pearson moment correlation matrix for various water quality parameters at borehole locations. The matrix provides a quantitative representation of the

relationships between these parameters, helping to identify which factors are more closely associated with one another and, consequently, which might have a greater influence on water quality.

The temperature, turbidity, pH, electrical conductivity (EC), chloride (Cl), fluoride (F), calcium carbonate ( $\text{CaCO}_3$ ), and several other ions (such as  $\text{Fe}^{2+}$ ,  $\text{Mg}^{2+}$ ,  $\text{Mn}^{2+}$ , and nitrate ( $\text{NO}_3^-$ )) are key indicators of water quality in the studied boreholes. The correlation matrix

allowed for the identification of parameters that either positively or negatively influence each other. These binary relationships can provide insights into water chemistry and inform decisions regarding water treatment and usage (Gandla *et al.*, 2024).

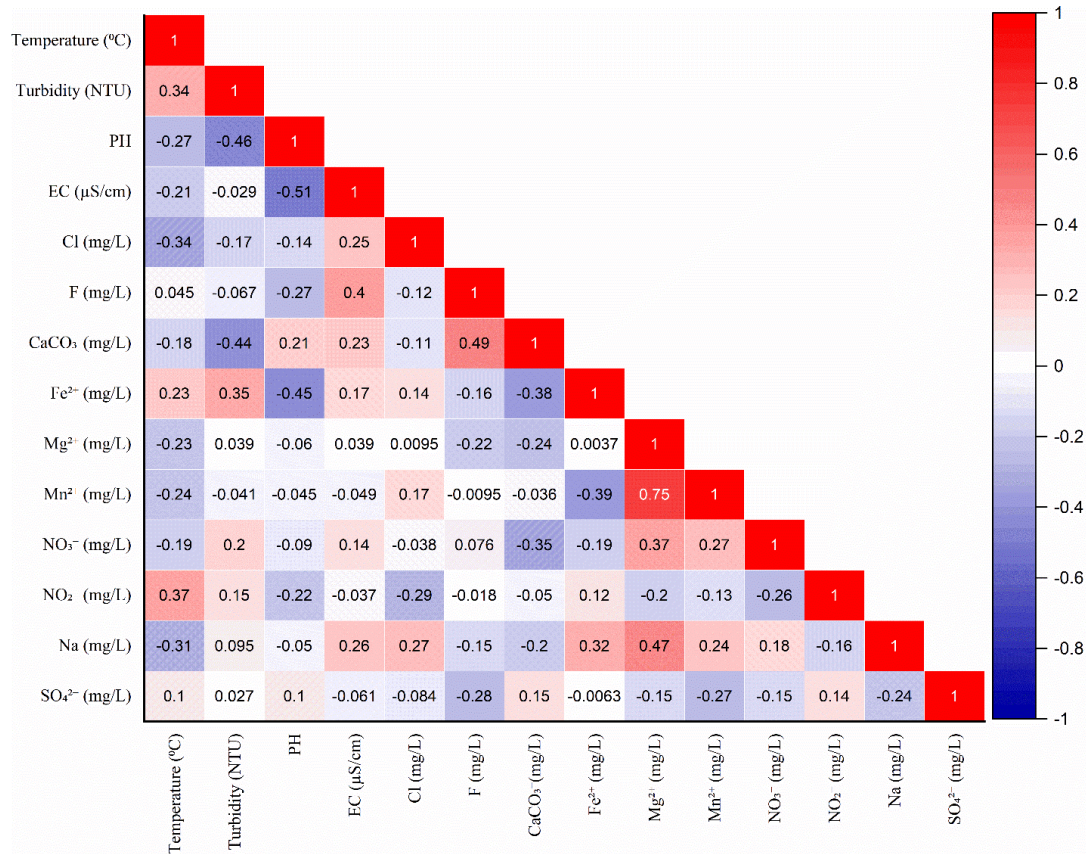


Figure 16: Pearson Moment Correlation Matrix of Water Quality Parameters for Borehole Locations

## 4.5 Hydrogeochemical Facies Classifications

### 4.5.1 Piper Diagram Analysis

The Piper diagram (Figure 17) was employed to evaluate the hydrochemical facies of groundwater samples collected from the boreholes. The cations and anions data, including sodium ( $\text{Na}^+$ ), magnesium ( $\text{Mg}^{2+}$ ), calcium carbonate ( $\text{CaCO}_3$ ), chloride (Cl), sulfate ( $\text{SO}_4^{2-}$ ), bicarbonate ( $\text{HCO}_3^-$ ), and carbonate ( $\text{CO}_3^{2-}$ ), were plotted to determine the dominant ion species and to classify the water types.

### 4.5.2 Durov Diagram Analysis

The Durov plot provides a comprehensive visualization of the hydrochemical characteristics of groundwater samples, facilitating the identification of water types, dominant ions, and potential geochemical processes. Figure 18 illustrates the distribution of groundwater samples across various zones in the Durov diagram, highlighting their chemical composition and interactions.

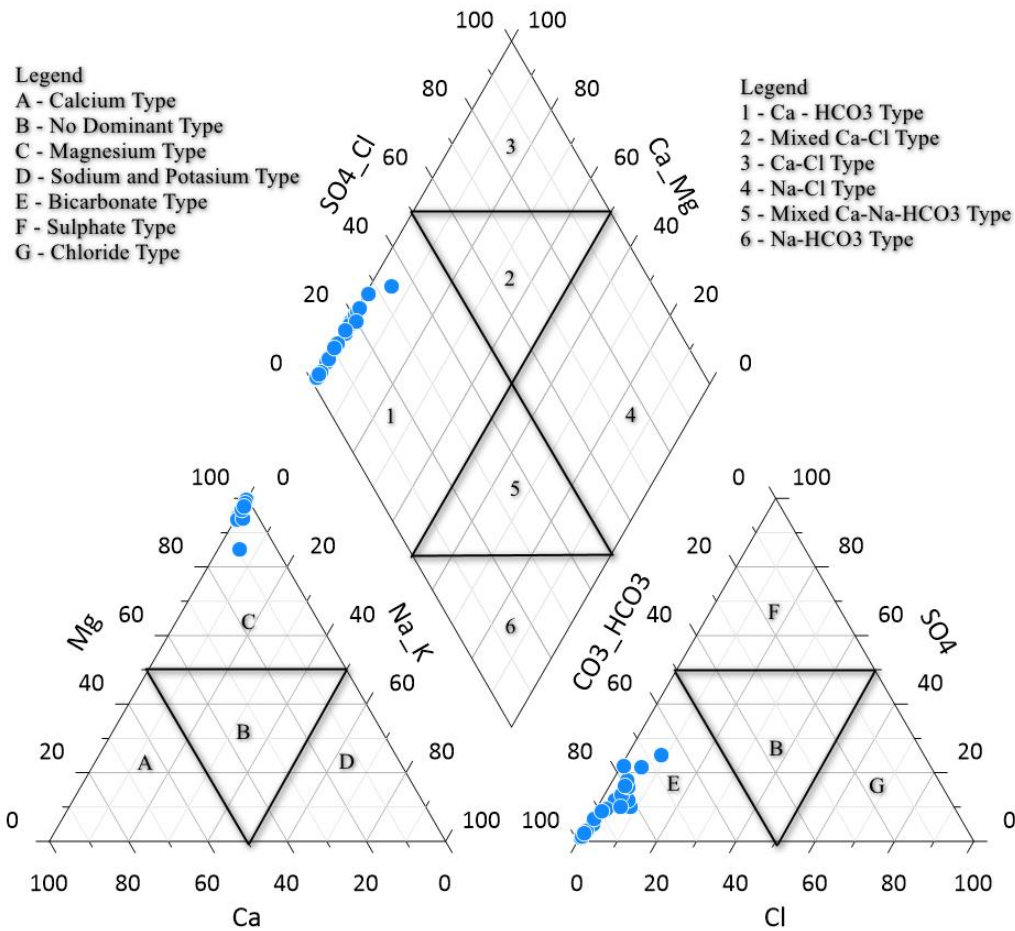


Figure 17: Hydrochemical Facies Characterization of Groundwater Samples Using Piper Plot

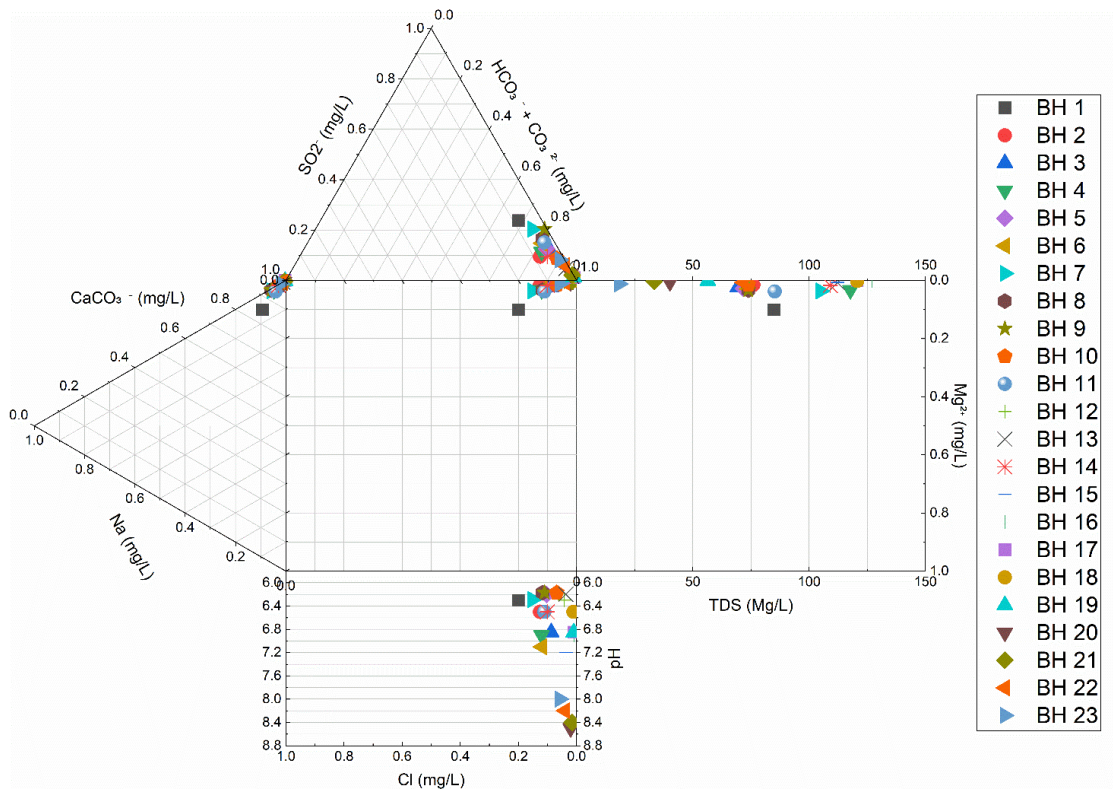


Figure 18: Hydrochemical Characterization of Groundwater Samples Using Durov Plot

## 5.0 Discussion of results

### 5.1 Physicochemical Parameters

The borehole water temperatures across the sampled locations ranged from 25.00°C in BH 4 (Ebom) to 30.60°C in BH 7 (Itigidi) in Table 2. The average temperature across all boreholes was 27.30°C, with a standard deviation of  $\pm 1.79$ . The spatial distribution, as illustrated in Figure 3, shows that higher temperatures were observed in southern regions, such as Itigidi and its surrounding areas.

The spatial distribution of turbidity levels, depicted in Figure 4, indicates a range from 14.20 NTU in BH 16 (Akugom, Ugep) to 22.00 NTU in BH 3 (Anong). The mean turbidity value for the sampled boreholes is 17.96 NTU.

The pH values across the sampled boreholes ranged from 6.17 in BH 10 (Etono) to 8.50 in BH 20 (Mkpani). The spatial spread is presented in Figure 6. The mean pH across the boreholes is 6.87, which falls within the ideal range of 6.0 to 8.5 recommended for irrigation purposes.

The EC values in the study area ranged from 28.67  $\mu\text{S}/\text{cm}$  in BH 23 (Ugep) to 198.50  $\mu\text{S}/\text{cm}$  in BH 16 (Akugom, Ugep). The average EC value for the boreholes is 133.43  $\mu\text{S}/\text{cm}$ , reflecting consistently low salinity and total dissolved solute (TDS) across the region. The distribution of EC in Figure 6 shows relative spread as low, moderate and high values in the study area,

The combined analysis of temperature, turbidity, pH, and electrical conductivity confirms that the borehole water in the study area is well-suited for irrigation and other purposes (Akpan *et al.*, 2013). The parameters assessed are within acceptable ranges for agricultural use, ensuring that water quality does not pose a constraint to crop productivity. Spatial trends observed across the parameters provide valuable insights into the underlying environmental and anthropogenic factors influencing water quality.

For the hydrochemical (major anions) parameters, the chloride concentration across the boreholes ranges from 0.25 mg/L in BH 9 (Agwuagune) to 5.10 mg/L in BH 2 (Adadama). The spatial map of chloride (Figure 7) highlights relatively low and uniform concentrations, with slightly elevated values in Adadama and Ogada. Chloride levels are well below the WHO guideline of 250 mg/L for drinking water, ensuring the absence of salinity concerns (Thomas *et al.*, 2020; George & Thomas, 2023). The mean chloride concentration is 1.74 mg/L, with a standard deviation of  $\pm 1.08$  mg/L, reflecting minimal variability.

Fluoride concentrations range from 0.03 mg/L in BH 21 (Nko) to 0.21 mg/L in BH 17 (Genong, Obioko-Ijiman). As illustrated in Figure 8, higher fluoride levels are observed in Genong and Ijiman-Ugep, while lower values are distributed across boreholes like Nko and Ababene. All fluoride concentrations fall significantly below the WHO limit of 1.5 mg/L, indicating no risk of fluorosis in humans or toxicity to plants (Chen *et al.*, 2021; George & Thomas, 2023b). The average fluoride concentration is 0.13 mg/L, with a standard deviation of  $\pm 0.05$  mg/L.

Nitrate concentrations exhibit notable variability, ranging from 0.10 mg/L in several boreholes, such as BH 5 (Ikpalegwa) and BH 6 (Imabana), to 2.00 mg/L in BH 13 (Isabang) and BH 15 (Ovukwa). The spatial map of nitrate (Figure 9) shows localized areas of elevated nitrate levels, particularly in Isabang and Ovukwa, which may be influenced by agricultural runoff or organic matter decomposition. The mean nitrate concentration is 0.91 mg/L, with a standard deviation of  $\pm 0.60$  mg/L. All nitrate values are well below the WHO limit of 50 mg/L for drinking water, ensuring no health or environmental risks (WHO, 2022).

Sulfate concentrations vary from 4.50 mg/L in BH 5 (Ikpalegwa) to 7.20 mg/L in BH 12

(Apiapum) and BH 22 (Ntankpo Ugep). The spatial map (Figure 10) reveals relatively higher sulfate concentrations in Apiapum and NtankpoUgep, with lower values in Ikpalegwa and nearby regions. The mean sulfate concentration is 5.85 mg/L, with a standard deviation of  $\pm 0.88$  mg/L. These values are significantly below the WHO guideline of 500 mg/L, reflecting excellent water quality for both irrigation and consumption (Gandla *et al.*, 2024).

Nitrite concentrations range from 0.01 mg/L in BH 4 (Ebom) to 1.10 mg/L in BH 9 (Agwuagune) in Table 1 illustrates the spatial distribution, with higher nitrite concentrations localized in Agwuagune, potentially due to partial denitrification or organic matter decomposition (Ibuot *et al.*, 2017). The average nitrite level is 0.16 mg/L, with a standard deviation of  $\pm 0.22$  mg/L. WHO recommends a maximum of 3 mg/L for nitrite in drinking water (WHO, 2022); thus, all values are within safe limits. Nitrite at these levels is unlikely to pose any threat to irrigation systems or plant health.

For hydrochemical parameter (major cations), the borehole data for  $\text{CaCO}_3$  ranged from 11.00 mg/L in Usumutong (BH 1) to 376.00 mg/L in Genong, Obioko-Ijiman (BH 17). The spatial map of  $\text{CaCO}_3$  (Figure 11 clearly illustrates the varying levels across different locations, with southern boreholes generally exhibiting higher concentrations of  $\text{CaCO}_3$  compared to northern sites. The mean concentration of  $\text{CaCO}_3$  across all boreholes was 134.71 mg/L, with a standard deviation of  $\pm 110.77$  mg/L, indicating significant spatial variability. These levels are classified as moderately hard to very hard water, with concentrations in certain areas surpassing WHO's recommended limits for drinking water (200 mg/L for calcium carbonate) but remaining within acceptable ranges for irrigation.

Iron concentrations in the water boreholes ranged from 3.05 mg/L in Genong, Obioko-Ijiman (BH 17) to 6.23 mg/L in Ababene (BH

11). The spatial map of Iron ( $\text{Fe}^{2+}$ ) in Figure 12 reveals that higher concentrations of iron are generally observed in the central and southern regions of the study area. The average concentration of  $\text{Fe}^{2+}$  across all boreholes was 4.44 mg/L, with a standard deviation of  $\pm 0.74$  mg/L. These values are above the WHO guideline for drinking water, which recommends an iron concentration of less than 0.3 mg/L for potable water (WHO, 2022).

Magnesium concentrations in the borehole water ranged from 0.10 mg/L in multiple locations such as BH 2 (Adadama) and BH 7 (Itigidi) to 0.49 mg/L in Ababene (BH 11). The spatial map of Magnesium ( $\text{Mg}^{2+}$ ) in Figure 13 illustrates a relatively uniform distribution of magnesium across the study area, with most values concentrated around 0.10 mg/L to 0.20 mg/L.

The average magnesium concentration was 0.16 mg/L, with a standard deviation of  $\pm 0.09$  mg/L. These concentrations are well within acceptable limits for both drinking water and irrigation. Manganese concentrations in the borehole water ranged from 0.10 mg/L in several boreholes such as BH 6 (Imabana) and BH 10 (Etono) to 0.32 mg/L in BH 4 (Ebom). The spatial map of Manganese ( $\text{Mn}^{2+}$ ) Figure 14 in shows a relatively uniform distribution across the study area, with slightly higher concentrations observed in the western and central regions. The average manganese concentration across all boreholes was 0.16 mg/L, with a standard deviation of  $\pm 0.07$  mg/L. These values are well within the permissible limits for both drinking water and irrigation as set by WHO.

Sodium concentrations in the borehole water ranged from 1.10 mg/L in multiple locations such as BH 1 (Usumutong) to 1.41 mg/L in Ebom (BH 4). The spatial map of Sodium ( $\text{Na}^+$ ) in Figure 15 indicates that sodium concentrations are relatively consistent across the study area, with only minor variations observed between different borehole locations. The mean concentration of sodium across all

boreholes was 1.14 mg/L, with a standard deviation of  $\pm 0.07$  mg/L. These concentrations are well within acceptable limits for both irrigation and drinking water, with sodium levels not posing a significant risk of salinization in the soil.

### 5.3 Correlation Matrix Analysis

In Figure 16, the temperature ( $^{\circ}\text{C}$ ) shows a moderate positive correlation with turbidity (0.335) and nitrate ( $\text{NO}_3$ ) levels (0.374). This suggests that higher temperatures may be associated with increased turbidity, potentially due to more suspended particles in the water at warmer temperatures, or it could reflect the presence of organic matter that contributes to both turbidity and elevated nitrate concentrations. The temperature's negative correlation with  $\text{Fe}^{2+}$  (-0.234) and  $\text{Mn}^{2+}$  (-0.235) indicates that higher temperatures may reduce the solubility of iron and manganese, thereby potentially decreasing their concentrations in the water.

Turbidity (NTU), which measures the cloudiness or haziness of the water, has a significant negative correlation with pH (-0.464) and a moderate positive correlation with both  $\text{Fe}^{2+}$  (0.354) and  $\text{Mn}^{2+}$  (0.038). The negative correlation with pH indicates that as turbidity increases, the pH of the water tends to decrease, which might be due to the presence of organic and inorganic acids that influence water acidity. The positive correlation with iron and manganese levels suggests that higher turbidity may be associated with increased levels of these metals, possibly due to contamination or leaching from surrounding soils and rocks.

pH levels in the borehole water show negative correlations with  $\text{Fe}^{2+}$  (-0.453),  $\text{Mn}^{2+}$  (-0.045), and  $\text{NO}_3^-$  (-0.090), indicating that as pH decreases (water becomes more acidic), the concentrations of these elements may increase. This is in line with the behavior of metals in water, where acidic conditions often result in higher solubility of metals such as iron and

manganese, which could pose risks to water quality and human health. Conversely, the negative correlations between pH and other parameters such as chloride (Cl) and sulfate ( $\text{SO}_4^{2-}$ ) further suggest that water chemistry changes as pH fluctuates, especially when pH drops.

The electrical conductivity (EC), which measures the water's ability to conduct electricity, is positively correlated with several ions, such as sodium (Na), chloride (Cl), and calcium carbonate ( $\text{CaCO}_3$ ). EC has a moderate positive correlation with nitrate ( $\text{NO}_3^-$ ) and phosphate (F), highlighting that higher concentrations of ions tend to correlate with higher EC values, suggesting that water with higher dissolved ions is more conductive. This relationship is important because increased EC can indicate the presence of various contaminants, including salts and metals, which can affect water quality and its suitability for use in agriculture or drinking.

Calcium carbonate ( $\text{CaCO}_3$ ) concentrations show a moderate positive correlation with fluoride (F) and magnesium ( $\text{Mg}^{2+}$ ), both of which are key indicators of water hardness. This reflects the fact that calcium carbonate, which contributes to water hardness, may occur alongside other ions such as magnesium and fluoride. Interestingly, the negative correlation between  $\text{CaCO}_3$  and  $\text{Fe}^{2+}$  (-0.383) further supports the idea that hard water may have lower concentrations of iron, potentially due to precipitation or other interactions in the water.

The concentrations of iron ( $\text{Fe}^{2+}$ ) and manganese ( $\text{Mn}^{2+}$ ) show weak to moderate correlations with several other water quality parameters, such as chloride (Cl) and nitrate ( $\text{NO}_3^-$ ). These correlations suggest that iron and manganese contamination in borehole water is often influenced by multiple factors, including changes in water temperature, pH, and other dissolved ions. The positive correlation between  $\text{Mn}^{2+}$  and magnesium ( $\text{Mg}^{2+}$ ) indicates that areas

with high levels of magnesium may also see elevated manganese levels, which could reflect shared sources of contamination, such as industrial runoff or soil erosion.

Nitrate ( $\text{NO}_3^-$ ), an important indicator of pollution from fertilizers and wastewater, shows weak correlations with other elements like fluoride and sulfate ( $\text{SO}_4^{2-}$ ). While nitrate levels correlate positively with temperature, they do not strongly correlate with most other major ions, suggesting that its presence is likely more related to specific pollution sources than to the overall mineral composition of the water.

The correlation matrix highlights several important relationships between water quality parameters in boreholes. Understanding these correlations is crucial for identifying potential sources of contamination and addressing the specific treatment needs for each water source. While several parameters show significant correlations, others, such as nitrate, fluoride, and sulfate, tend to have weaker associations with other ions, indicating that they may be influenced by different environmental or anthropogenic factors. By analyzing these correlations, water quality management strategies can be better tailored to the specific needs of each borehole.

## 5.4 Hydrogeochemical Facies Classifications

### 5.4.1 Piper Diagram Analysis

In Figure 17, the results of Piper diagram revealed that the majority of the groundwater samples fall into the magnesium-bicarbonate type, specifically classified as Ca- $\text{HCO}_3$  facies. This indicates that bicarbonates are the dominant anions in the groundwater system, with magnesium and calcium being the primary cations (Odong *et al.*, 2024). Such hydrochemical characteristics are typical of water samples influenced by rock-water interactions, particularly dissolution of carbonate minerals like calcite and dolomite in the aquifer system.

Groundwater samples from boreholes BH 12, BH 13, BH 15, BH 16, BH 17, BH 18, and BH 19 demonstrated a pronounced enrichment in bicarbonate ( $\text{HCO}_3^-$ ) with elevated calcium ( $\text{Ca}^{2+}$ ) concentrations. These samples represent a strong Ca- $\text{HCO}_3$  signature, consistent with carbonate rock dissolution processes (Sikakwe & Eyoung, 2022). Similarly, samples with lower  $\text{HCO}_3^-$  values, such as BH 7, BH 8, and BH 9, reflect less interaction with carbonate minerals and a relatively diluted geochemical composition.

The dominance of bicarbonate ions indicates that the groundwater is fresh and predominantly influenced by meteoric water recharge, with minimal impact from anthropogenic pollution or saltwater intrusion (Akpan *et al.*, 2013). The presence of magnesium further suggests contributions from dolomite dissolution or weathering of silicate minerals in the aquifer.

The Piper plot effectively illustrates the hydrochemical evolution of the water system, highlighting a uniform dominance of magnesium and bicarbonate ions across the sampled boreholes. This supports the classification of the water as predominantly Ca- $\text{HCO}_3$  type, reflecting the geogenic control of groundwater chemistry in the study area.

### 5.4.2 Durov Diagram Analysis

The analysis in Figure 18 confirmed that most groundwater samples belong to the Ca-Mg- $\text{HCO}_3$  water type, signifying a strong influence of carbonate dissolution. Some boreholes displayed ion exchange characteristics, where  $\text{Ca}^{2+}$  was replaced by  $\text{Na}^+$ , which is indicative of cation exchange processes occurring within the aquifer matrix over extended residence times.

The pH values, ranging from 6.17 to 8.5, suggest that the groundwater is mildly acidic to slightly alkaline. This trend aligns with the dominant bicarbonate buffering system in the aquifers, which neutralizes acidity. The low concentrations of sulfate ( $\text{SO}_4^{2-}$ ) and chloride ( $\text{Cl}^-$ ) in most samples indicate limited

anthropogenic contamination or minimal evaporative influences. However, samples with higher  $\text{Cl}^-$  concentrations, such as BH 7 and BH 16, may reflect localized contamination or groundwater mixing with deeper aquifers.

Samples like BH 16 and BH 17, with their high total dissolved solids (TDS), are indicative of longer residence times or interaction with mineral-rich geological formations. These samples are positioned closer to the upper right of the Durov diagram, signifying the transition to more mineralized water. The geochemical processes, such as dissolution, ion exchange, and mixing, collectively shape the observed water chemistry patterns in the area.

The Durov plot effectively delineates groundwater facies and provides insights into the governing hydrochemical processes, emphasizing the bicarbonate-rich nature of the aquifer system in the study area.

### 5.6 Implications for Public Health

The presence of high nitrate levels in certain locations poses a risk of methemoglobinemia (blue baby syndrome), especially among infants. Prolonged exposure to high iron and manganese concentrations can result in neurological complications. To mitigate these risks, groundwater sources should undergo periodic monitoring, and suitable treatment methods such as aeration and filtration should be employed.

### 5.7 Management and Policy

The geochemical analysis of groundwater in Central Cross River State is vital for water quality and public health. A structured policy framework ensures sustainability through continuous monitoring, pollution control, and compliance with World Health Organization (WHO) and Nigerian Standard for Drinking Water Quality (NSDWQ) standards. Key strategies include groundwater protection zones, eco-friendly farming, public awareness on waterborne diseases, and household water treatment. Sustainable management involves Integrated Water Resource Management

(IWRM), alternative water sources, and public-private partnerships for infrastructure development.

Implementation of regular groundwater monitoring programs to track changes in water chemistry.

## 6.0 Conclusion

This study provides a comprehensive assessment of the geochemical characteristics of groundwater within the Ikom-Mamfe Embayment, highlighting the spatial variability of key physicochemical parameters and their implications for public health. The findings reveal that groundwater quality is largely influenced by both natural lithological factors and anthropogenic activities, with contamination sources primarily linked to agricultural runoff, waste disposal, and industrial effluents.

The presence of elevated nitrate levels in some locations underscores the impact of human-induced contamination, necessitating urgent mitigation measures to protect public health. Similarly, the occurrence of high iron and manganese concentrations, attributed to geogenic sources, calls for targeted water treatment solutions to ensure potable water standards are met.

The hydrogeochemical analysis, supported by Piper and Durov diagrams, has provided valuable insights into the groundwater facies and ion exchange processes within the study area. Correlation matrix analysis further reinforces the significant relationships between various water quality parameters, aiding in the identification of key geochemical processes controlling groundwater composition.

Given the observed variability in water quality, this study strongly advocates for monitoring and management processes to sustain all-season groundwater availability (Ekanem *et al.*, 2020, 2024; George *et al.*, 2017). Regular groundwater monitoring programs should be established to

track temporal changes in water chemistry and detect emerging contamination threats. In addition, strict pollution control regulations must be implemented to minimize the infiltration of agricultural and industrial contaminants into groundwater resources. Developing cost-effective water treatment methods tailored to specific contamination issues, such as aeration and filtration techniques to reduce iron and manganese concentrations, is essential. Furthermore, strengthening community engagement and public health education programs will help raise awareness of groundwater contamination risks and promote safe water use practices. Lastly, integrating groundwater protection into broader environmental and urban planning policies is crucial to ensuring sustainable water resource management.

In conclusion, this study highlights the need for a multi-faceted approach to groundwater management that balances scientific assessment, policy enforcement, and community participation. Future research should focus on long-term hydrogeochemical monitoring, isotope studies to trace groundwater recharge sources, and the development of adaptive strategies for climate-induced changes in water quality. Addressing these challenges will enhance the resilience of groundwater resources and ensure the continued availability of safe drinking water for communities in Central Cross River State.

### References:

- Akpan A. E, Ugbaja, A. N. & George, N. J. (2013) Integrated geophysical, geochemical and hydrogeological investigation of shallow groundwater resources in parts of the Ikom-Mamfe Embayment and the adjoining areas in Cross River State, Nigeria. *Environ. Earth Sci*, 70 (3). 1435–1456, Doi. 10.1007/s12665-0132232-3.
- Akpan, A. E., Ugbaja, A. N., Okoyeh, E.I. & George, N.J, (2018), Assessment of spatial distribution of contaminants and their levels in soil and water resources of Calabar, Nigeria using geophysical and geological data, *Environmental Earth Sciences*, 77: 13,10.1007/s12665-017-7189-1
- American Public Health Association (APHA). (2017). Standard Methods for the Examination of Water and Wastewater. Washington, D.C.: APHA.
- Bassey CE, Eminue, O. O. & Ajonina HN (2013) Stratigraphy and depositional environments of the Mamfe formation and its implication on the tectono-sedimentary evolution of the Ikom-Mamfe Embayment, West Africa. *Cent Eur J Geosci* 5(3):349–406
- Chen J, Gao Y, Qian H, Ren W. & Qu W (2021) Hydrogeochemical evidence for fluoride behavior in groundwater and the associated risk to human health for a large irrigation plain in the Yellow River Basin. *Sci Total Environ* 800:149428. <https://doi.org/10.1016/j.scitotenv.2021.149428>
- Duoxun X, Peiyue L, Xin C, Shengfei Y. & Pei F. G. (2023) Major ion Hydrogeochemistry and health risk of groundwater nitrate in selected rural areas of the Guanzhong Basin, China. *Hum Ecol Risk Assess Int J*. <https://doi.org/10.1080/10807039.2022.2164246>
- Durov, S. A. (1948). Natural Waters and Their Evolution. *Geological Review*, 43, 23-31.
- Ekanem, A. M., Akpan, A., George, N. J. & Thomas, J. E. (2021). Appraisal of protectivity and corrosivity of surficial

- hydrogeological units via geo-sounding measurements. *Environ Monit Assess*, 193:718. <https://doi.org/10.1007/s10661-021-09518-9>
- Ekanem, A. M., George, N. J., Thomas, J. E. & Nathaniel, E. U. (2020). Empirical Relations Between Aquifer Geohydraulic – Geoelectric Properties Derived from Surficial Resistivity Measurements in Parts of Akwa Ibom State, Southern Nigeria. *Natural Resources Research* 29(4), 2635-2646. <https://doi.org/10.1007/s11053-019-09606-1>.
- Ekanem, A. M., George, N. J., Thomas, J. E., Udo, I. G. (2024). Geophysical investigation of aquifer flow unit characteristics in northern parts of Akwa Ibom State, Southern Nigeria. *Results in Earth Sciences*, 2, 100017. <https://doi.org/10.1016/j.rines.2024.100017>
- Ekwere, A. S., & Ekwueme, B. N. (2016). Hydrogeochemical assessment of groundwater in Central Cross River State, Nigeria. *Journal of African Earth Sciences*, 117, 142-153.
- Etesin, U. M, George, N. J, Ogbonna, I. J. & Akpan, I. O. (2023). Source Identification and Variation in the chemical Composition of Rainwater in the Coastal and Industrial Areas: A Case Study of Ikot Abasi, South-Eastern Nigeria. *Earth Sciences*, 7(1): 55-63.
- Gandla, S., Umrikar, B., George, N.J. & Gupta, G. (2024) Geochemical assessment of groundwater quality for domestic, irrigation and industrial purposes: a tool for environmental monitoring and assessment in a semiarid region of eastern Maharashtra, India, *Discover Water*, <https://doi.org/10.1007/s43832-024-00158-x>
- George, N. J., Ekanem, A. M., Thomas, J. E. & Ekong, S. A., (2021). Mapping depths of groundwater - level architecture: implications on modest groundwater - level declines and failures of boreholes in sedimentary environs. *Acta Geophysica*, 69: 1919–1932. <https://doi.org/10.1007/s11600-021-00663-w>
- George, N. J. & Thomas, J. E. (2023a) Typification of coastal depositional lithofacies with isophysical and isochemical hydro-sand beds via stratigraphic modified Lorenz plots (SMLP): geohydrodynamical implications and valorization of hydrogeological units. *Acta Geophys.* <https://doi.org/10.1007/s11600-023-01160-y>
- George, N.J. & Thomas, JE. (2023b) Groundwater potential and quality assessments of a coastal environment: a case study of the location of Federal University of Technology Ikot Abasi (FUTIA), Akwa Ibom State, Nigeria, *Journal of Coastal Conservation*, 27 (4), <https://doi.org/10.1007/s11852-023-00956-w>
- Hem, J. D. (1985). Study and Interpretation of the Chemical Characteristics of Natural Water. U.S. Geological Survey Water-Supply Paper 2254.
- Ibanga Jewel I. & George N. J., (2016) Estimating geohydraulic parameters, protective strength, and corrosivity of hydrogeological units: a case study of ALSCON, Ikot Abasi, southern Nigeria,

- Arabian Journal of Geosciences*, 9(5), 1-16.
- Ibuot, J. C., Okeke, F.N, George, N.J & Obiora, D. N. (2017), Geophysical and physicochemical characterization of organic waste contamination of hydrolithofacies in the coastal dumpsite of Akwa Ibom State, southern Nigeria, *Water Science & Technology: Water Supply*, 17 (6): 1626-1637, doi: 10.2166/ws.2017.066.
- Inim I. J., Udosen N. I., Tijani M. N., Afia U. E., George N. J. (2020). Time-lapse electrical resistivity investigation of seawater intrusion in coastal aquifer of Ibeno, Southeastern Nigeria, *Applied Water Science*, Germany, 10, 232 (2020), <https://doi.org/10.1007/s13201-020-01316-x>
- Inyang, N.E, George, N.J., Ehibor, I.U., Ekot, A.E.& Udoh, I.G. (2023). Integrated valorization of MSW incursion into water resources: a tool for environmental monitoring and assessment near dumpsite areas, Akwa Ibom State, Nigeria. <https://doi.org/10.21203/rs.3.rs-3492331/v1>
- Obiora, D. N., Ibuot, J. C., George, N. J., & Offiah, S. U. (2016). Delineation of groundwater saturation indicators and their distributions in the complex argillaceous geological units of Ezza north local government area of Ebonyi state, Nigeria. *Current Science*, 110(4), 701 – 708
- Odong, P.O., Ebong, E.D., Awak, E.A., Ojong, R.A. & Umera, R.B. (2024) Integrated geophysical and hydrogeochemical characterization of groundwater vulnerability conditions in part of Ikom-Mamfe Embayment, southeastern Nigeria. *Sustain. Water Resour. Manag.* 10, 120. <https://doi.org/10.1007/s40899-024-01094-3>
- Okon, E. B., Udo, I. A., & Udoh, P. D. (2018). Groundwater geochemistry and contamination assessment in Ikom-Mamfe Embayment, Nigeria. *Environmental Geochemistry and Health*, 40(5), 2101-2116.
- Piper, A. M. (1944). A Graphic Procedure in the Geochemical Interpretation of Water Analyses. *Transactions of the American Geophysical Union*, 25, 914-928.
- Sikakwe G. U. & Eyong, G.A. (2022) Groundwater flow and geochemical processes affecting its quality in the basement (Oban Massif) and sedimentary (Mamfe Embayment) environments, southeastern Nigeria, *Journal of African Earth Sciences*, 188, <https://doi.org/10.1016/j.jafrearsci.2022.104467>
- Thomas, J. E. George, N. J. & Ekanem, A. M. & E. E. Nsikak (2020). Electrostratigraphy and hydrogeochemistry of hyporheic zone and water-bearing caches in the littoral shorefront of Akwa Ibom State University, Southern Nigeria, *Environ. Monit Assess.*, 192 (8) 1-19 <https://doi.org/10.1007/s10661-020-08436-6>
- Udosen, N. I., Ekanem, A. M.& George N. J. (2024). Appraisal of Flood-Prone Litho-Stratigraphic Units Via Geo-Electrical Technology. *Malaysian Journal of Geosciences (MJG)*, 8(1) (2024) 26-37. DOI: <http://doi.org/10.26480/mjg.01.2-024.26.37>
- Uka, N. K., Nfor, B., & Eze, E. O. (2019). Isotopic and hydrogeochemical

characteristics of groundwater in Southeastern Nigeria. *Hydrology Journal*, 8(2), 78-92.

Umoh, J. A., George, N. J., Ekanem, A. M., Thomas, J. E. & Emah, J. B. (2022a). Approximate delineation of groundwater yield capacity and vulnerability via secondary geo-electric indices and rock-water interaction hydrodynamic coefficients in a coastal environment. *Researchers Journal of Science and Technology*, 2(3): 28 – 54

Umoh, J. A., George, N. J., Ekanem, A.M. & Emah, J. B. (2022b). Characterization of hydro-sand beds and their hydraulic flow units by integrating surface measurements and ground truth data in parts of the shorefront of Akwa Ibom State, Southern Nigeria. *Int. J. Energy Water Resources*. <https://doi.org/10.1007/s42108-022-00215-y>

World Health Organization (WHO). (2022). *Guidelines for Drinking-Water Quality* (4th ed.). Geneva: WHO.